JVI Journals.ASM.org

Oligomerization of Mumps Virus Phosphoprotein

Adrian Pickar,[a] Andrew Elson,[a] Yang Yang,[a] Pei Xu,[a]* Ming Luo,[b] Biao He[a]

Department of Infectious Diseases, College of Veterinary Medicine, University of Georgia, Athens, Georgia, USA[a]; Department of Chemistry, Georgia State University, Atlanta, Georgia, USA[b]

ABSTRACT

The mumps virus (MuV) genome encodes a phosphoprotein (P) that is important for viral RNA synthesis. P forms the viral RNA-dependent RNA polymerase with the large protein (L). P also interacts with the viral nucleoprotein (NP) and self-associates to form a homotetramer. The P protein consists of three domains, the N-terminal domain (P_N), the oligomerization domain (P_O), and the C-terminal domain (P_C). While P_N is known to relax the NP-bound RNA genome, the roles of P_O and P_C are not clear. In this study, we investigated the roles of P_O and P_C in viral RNA synthesis using mutational analysis and a minigenome system. We found that P_N and P_C functions can be *trans*-complemented. However, this complementation requires P_O, indicating that P_O is essential for P function. Using this *trans*-complementation system, we found that P forms parallel dimers (P_N to P_N and P_C to P_C). Furthermore, we found that residues R231, K238, K253, and K260 in P_O are critical for P's functions. We identified P_C to be the domain that interacts with L. These results provide structure-function insights into the role of MuV P.

IMPORTANCE

MuV, a paramyxovirus, is an important human pathogen. The P protein of MuV is critical for viral RNA synthesis. In this work, we established a novel minigenome system that allows the domains of P to be complemented in *trans*. Using this system, we confirmed that MuV P forms parallel dimers. An understanding of viral RNA synthesis will allow the design of better vaccines and the development of antivirals.

Mumps virus (MuV) is a human pathogen of the *Rubulavirus* genus of the *Paramyxoviridae* family that causes an acute infection with symptoms ranging from parotitis to mild meningitis and severe encephalitis (1). The nonsegmented, negative-stranded RNA genome of MuV contains 15,384 nucleotides and encodes nine viral proteins (1). The viral RNA is encapsidated by the nucleoprotein (NP), and this helical nucleocapsid (RNP) functions as the template for viral RNA synthesis. Together, the large protein (L) and the phosphoprotein (P) make up the viral RNA-dependent RNA polymerase (vRdRp) (2). The enzymatic activities of the L protein involve the initiation, elongation, and termination of RNA synthesis, as well as mRNA capping (3). While P is not known to have intrinsic enzymatic activity, P is an essential cofactor of the polymerase. P oligomerizes by itself and forms complexes with L, NP, and RNP. It is thought that P docks the vRdRP to RNP (4).

The P proteins of paramyxoviruses are modular and consist of N-terminal (P_N), oligomerization (P_O), and C-terminal (P_C) domains with flexible linkers between adjoining domains. The self-association of P is observed throughout negative-stranded RNA viruses (NSVs). The oligomerization domain of Sendai virus (SeV) P was the first to be crystallized, and those studies revealed a parallel coiled-coil tetramer (5, 6). The self-association of P is required for transcriptional activity, and the binding site for SeV L was found to neighbor the oligomerization region (5, 7–9). Tetrameric P structures have also been observed for other paramyxoviruses, with crystallization of the P oligomerization domains being found for measles virus, human metapneumovirus, and mumps virus (10–16).

The P protein of vesicular stomatitis virus (VSV), a member of the *Rhabdoviridae* family, forms a dimer consisting of two parallel α helices that are held together through hydrophobic interactions (17). Oligomerization of VSV P is also needed for P activity, as observed by a VSV minigenome assay (18, 19). The crystal structure of the rabies virus P dimerization domain reveals that each monomer consists of a helical hairpin between two α helices that permits interactions between the N-terminal helix of one monomer and the C-terminal helix of the other monomer (20). The N-terminal domain of rabies virus P interacts with the nascent NP and L, whereas the C-terminal domain binds to RNP (21–23). This structural difference may be important for rabies virus P function since the N-terminal and C-terminal domains of rabies virus are positioned on the same side, whereas these domains are at opposite ends of the oligomerization domains for VSV and SeV.

A C-terminal nucleocapsid-binding domain is found in numerous paramyxovirus P proteins (24–26). The last 49 amino acids (aa) of MuV P (aa 343 to 391) were found to directly mediate binding to the nucleocapsid through their interaction with the assembly domain of NP (27). This nucleocapsid-binding domain is conserved, but MuV P is unique in that the N-terminal domain also binds to the nucleocapsid (16). Electron microscopy revealed uncoiling of the helical nucleocapsid by the N-terminal domain of P, which resulted in enhanced viral RNA synthesis in a minigenome system (28). The crystal structure of the oligomerization

Received 5 July 2015 **Accepted** 17 August 2015

Accepted manuscript posted online 26 August 2015

Citation Pickar A, Elson A, Yang Y, Xu P, Luo M, He B. 2015. Oligomerization of mumps virus phosphoprotein. J Virol 89:11002–11010. doi:10.1128/JVI.01719-15.

Editor: D. S. Lyles

Address correspondence to Biao He, bhe@uga.edu.

* Present address: Pei Xu, Microbiology Department, University of Chicago, Chicago, Illinois, USA.

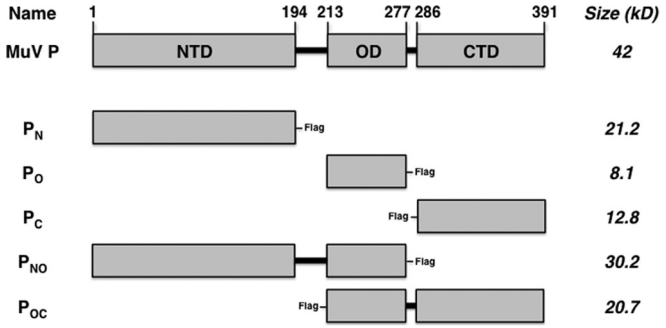

FIG 1 Schematic representation showing deletion mutants of MuV P. The amino acid residues for P_N, P_O, and P_C are provided. Mutant names correspond to the domains included in the P deletion mutants, and approximate sizes are provided. The terminal Flag tag locations are included for each mutant. NTD, N-terminal domain; OD, oligomerization domain; CTD, C-terminal domain.

domain (defined as residues 213 to 277) revealed two pairs of parallel α helices that are antiparallel to each other, which positions two N-terminal and two C-terminal domains on each end of the oligomerization domain (16). This antiparallel configuration is unique among P proteins of all nonsegmented negative-stranded RNA viruses.

In this study, we developed a novel minigenome system in which the functional domains of P can be studied using *trans*-complementation. Using this system, we have determined the configuration of the MuV P dimer and tetramer.

MATERIALS AND METHODS

Molecular cloning. The plasmids used in this work were constructed using standard molecular cloning techniques. The construction details and sequence files of the plasmids are available upon request. The NP, P, and L genes of the $MuV^{Iowa/US/06}$ strain were cloned into the pCAGGS expression vector (29). An MuV minigenome plasmid containing *Renilla* luciferase (R-Luc) (BH526/pMG-RLuc) and a plasmid containing firefly luciferase (FF-Luc) (pFF-Luc) were described previously (30). P truncations with Flag epitope tags are defined as P_N (aa 1 to 194-Flag), P_O (aa 213 to 277-Flag), P_C (Flag-aa 286 to 391), P lacking the C-terminal domain (P_{NO}; aa 1 to 277-Flag), and P lacking the N-terminal domain (P_{OC}; Flag-aa 213 to 391). P chimeric truncations with Flag epitope tags are defined as N_{MuV}-O_{PIV5} (aa 1 to 212 of MuV-aa 213 to 278 of parainfluenzavirus 5 [PIV5]-Flag), O_{PIV5}-C_{MuV} (Flag-aa 213 to 278 of PIV5-aa 278 to 391 of MuV), N_{PIV5}-O_{MuV} (aa 1 to 212 of PIV5-aa 213 to 277 of MuV-Flag), and O_{MuV}-C_{PIV5} (Flag-aa 213 to 277 of MuV-aa 279 to 391 of PIV5). The MuV L deletion mutant consisting of domains I through III ($L_{dI\text{-}III}$) with a hemagglutinin (HA) tag is defined as $L_{dI\text{-}III}$ aa 1 to 914-HA.

Cell culture and transfections. 293T cells were maintained in Dulbecco's modified Eagle medium (DMEM) with 5% fetal bovine serum (FBS) and 1% penicillin-streptomycin (P/S) (Mediatech Inc., Manassas, VA). BSRT7 cells were maintained in DMEM supplemented with 10% FBS, 1% P/S, 10% tryptose phosphate broth (TPB), and 400 μg/ml G418 sulfate antibiotic (Mediatech Inc.). All cell lines were incubated at 37°C with 5% CO_2 and passed at an appropriate dilution 1 day prior to use to achieve 80% to 90% confluence upon transfection. Cells were transfected using the JetPRIME transfection reagent (Polyplus Transfection Inc., New York, NY) following the manufacturer's protocols.

MuV minigenome system and dual-luciferase assay. The MuV minigenome system used in this study was described previously (30). Increasing amounts (0, 10, 20, 40, 80, 160, or 320 ng) of total P or P-domain truncations were transfected along with NP (25 ng), L (500 ng), pMG-RLuc (100 ng), and pFF-Luc (1 ng) into BSRT7 cells. The empty pCAGGS vector was used to normalize the amount of transfected DNA per sample. After 48 h, 2/5 of the lysate from each well was used to carry out the dual-luciferase assay according to the manufacturer's protocol (Promega, Madison, WI), and light intensity was detected using a GloMax 96 micro-

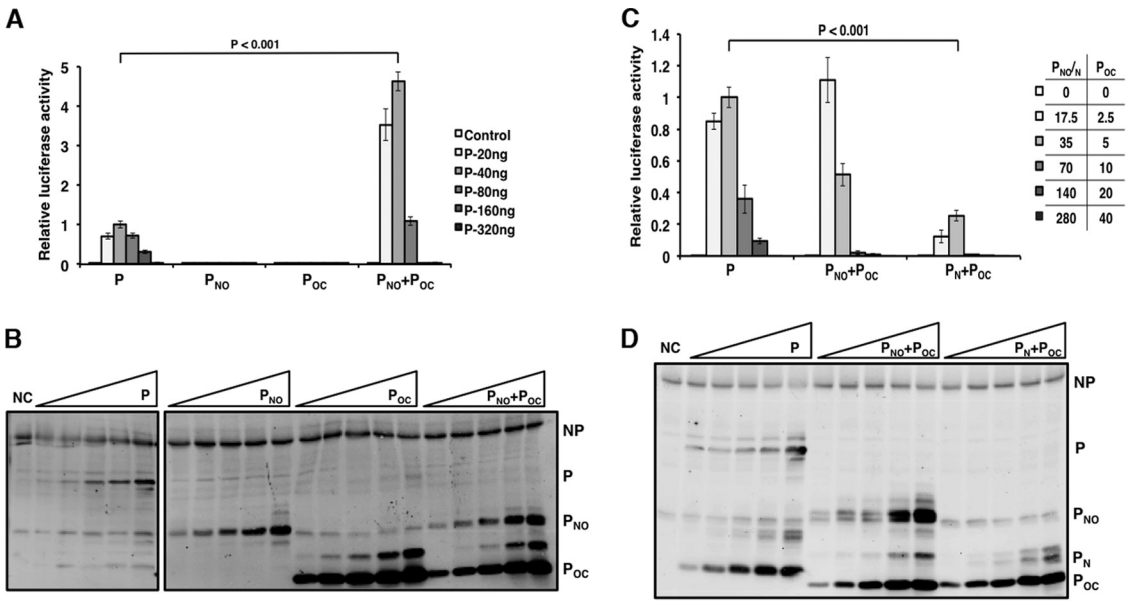

FIG 2 *trans*-Complementation of P in minigenome system. (A) Minigenome activity of P, P_{NO}, and P_{OC}. Increasing amounts of P or P deletion mutants were transfected together with other plasmids as described in Materials and Methods. For P_{NO}-P_{OC}, the amount of each deletion mutant transfected was one-half of the total amount of P transfected. *Renilla* luciferase was the reporter gene in the minigenome, and firefly luciferase expression was used as a transfection control. The minigenome activity was measured and normalized as the ratio of *Renilla* luciferase activity to firefly luciferase activity (relative luciferase activity). (C) Minigenome activity of P, P_N, P_{NO}, and P_{OC}. Increasing amounts of P or P deletion mutants were used. *P* values were calculated using Student's *t* test. Error bars represent the SEMs of data from six replicates. (B and D) Immunoblotting was performed to detect the expression levels of NP, P, and the P deletion mutants. Lanes NC, control.

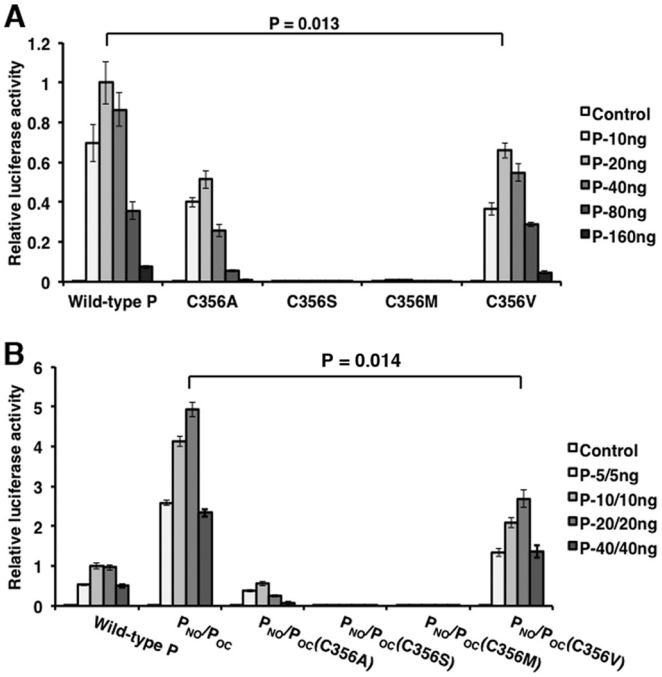

FIG 3 Mutation analysis of cysteine residue 356 of P. Residue C356 in full-length P and P_{OC} was mutated to alanine, serine, methionine, and valine and tested in the minigenome system. Increasing amounts of P or P deletion mutants were transfected together with other plasmids as described in Materials and Methods. The amounts transfected are provided in each graph. *P* values were calculated using Student's *t* test. Error bars represent the SEMs of data from six replicates.

plate luminometer (Promega). Relative luciferase activity was defined as the ratio of R-Luc activity to FF-Luc activity. Six replicates of each sample were used to compare the peak activity of each P mutant to that of wild-type P. Aliquots of cell lysates from the minigenome system were used for Western blot analysis. Mouse monoclonal anti-MuV NP and anti-MuV P antibodies and anti-Flag (M2 clone) antibody (Sigma-Aldrich, St. Louis, MO) were used together to detect the expression of NP, P, and P truncations, respectively.

Cysteine residue replacement and oligomer orientation determination. 293T cells were transfected with 1 μg of P_{NO} or P_{OC} containing cysteine mutations. After 24 h, the cells were lysed with whole-cell extraction buffer (WCEB; 50 mM Tris-HCl [pH 8.0], 280 mM NaCl, 0.5% NP-40, 0.2 mM EDTA, 2 mM EGTA, 10% glycerol) with a mixture of protease inhibitors as previously described (31). Prior to lysis, iodoacetamide (25 mM) was added to WCEB where specified. Cleared lysates were divided into equal fractions, mixed with a one-half volume of 3× SDS loading buffer containing dithiothreitol (DTT; reducing conditions) or not containing DTT (nonreducing conditions), and heated at 95°C for 5 min. Samples were resolved in 12.5% SDS-polyacrylamide gels and transferred to a polyvinylidene difluoride membrane (GE Healthcare, Piscataway, NJ).

Immunoblotting was performed as previously described (19). The membrane was blocked with enhanced chemiluminescence prime blocking agent (GE Healthcare Life Sciences, Piscataway, NJ), incubated with mouse anti-Flag (1:1,000 dilution) followed by incubation with goat Cy3-labeled anti-mouse IgG secondary antibody (1:2,500 dilution; KPL, Gaithersburg, MD), and scanned using a Typhoon 9700 imager (GE Healthcare Life Sciences).

Coimmunoprecipitation. To determine the P domains that interact with L, 6-well plates of 293T cells were transfected with 2 μg of P truncations with 3 μg of L_{dI-III}. At 18 h posttransfection (hpt), the cells were starved with DMEM lacking cysteine-methionine and then labeled with 36.4 μCi/ml ^{35}S-EasyTag Express35S protein labeling mix (PerkinElmer, Waltham, MA) for 4 h. The cells were then lysed with WCEB, and the lysate was precleared with recombinant protein G-Sepharose 4B conjugate (Invitrogen) for 1 h at 4°C and was then subjected to immunoprecipitation (IP) using recombinant protein G-Sepharose 4B conjugate and mouse anti-Flag or mouse anti-HA (Sigma-Aldrich). The IP products were washed with WCEB and resolved by 12.5% SDS-polyacrylamide gels. The gels were fixed (20% methanol, 7% acetic acid) and dried, and the proteins were visualized using a Typhoon 9700 imager (GE Healthcare).

Statistical analysis. Statistical analysis was performed using GraphPad Prism (version 5.00) software for Windows (GraphPad Software, San Diego, CA). Student's *t* test was used to calculate *P* values.

RESULTS

Functional activity of P domains. The MuV P protein contains an N-terminal domain (P_N), an oligomerization domain (P_O), and a C-terminal domain (P_C) which are connected with flexible linker regions. To determine the roles of these domains, a series of truncations was generated (Fig. 1). To examine the role of the individual P domains in viral RNA synthesis in the absence of viral infection, these deletion mutants were tested in the MuV minigenome system that has been previously described (30). A range of concentrations of the P plasmids was used to obtain the maximal minigenome activity since expression levels varied between the P domains. Previously, we showed that the individual domains do not maintain the P function in the MuV minigenome system (28). P truncations lacking the N-terminal domain or the C-terminal domain also had no activity (Fig. 2A). When P_{NO} and P_{OC} were transfected together in equal amounts, the luciferase activity was detected and was significantly greater than that of full-length P (Fig. 2A). The expression levels of P and NP were determined using immunoblotting (Fig. 2B). These results suggest that all P domains are required for P function. Most interestingly and importantly, P_{NO} and P_{OC} can *trans*-complement each other to restore the biological activity of P.

We previously found that addition of P_N with full-length P resulted in enhanced minigenome activity due to the role of the N-terminal domain in inducing uncoiling of the nucleocapsid (28). To determine whether *trans*-complementation requires the oligomerization domain, the N-terminal domain alone was transfected with P_{OC} and tested in the minigenome system. Transfection of P_N with P_{OC} resulted in some activity; however, the luciferase activity was significantly less than that of full-length P (Fig. 2C). The expression levels of P and NP were determined using immunoblotting (Fig. 2D). A lower ratio of P_{OC} was used due to the higher level of expression of the plasmid carrying this construct. These results suggest that self-oligomerization via P_O is required for functional *trans*-complementation of P in viral transcription and replication. The fact that P_N and P_C can *trans*-complement each other indicates that they indeed likely form functional domains.

P oligomerizes to form parallel dimers. Crystal structure analysis of P_O shows the formation of a tetramer consisting of two pairs of parallel α helices that are antiparallel to each other (16). This is unique among known paramyxovirus P proteins. To determine the preferential α-helical orientation during P dimerization, cysteine residues were strategically incorporated into the P protein for disulfide bond cross-linking. However, wild-type P contains one natural cysteine residue at amino acid 356 in the C-terminal domain. To avoid potential interference from this

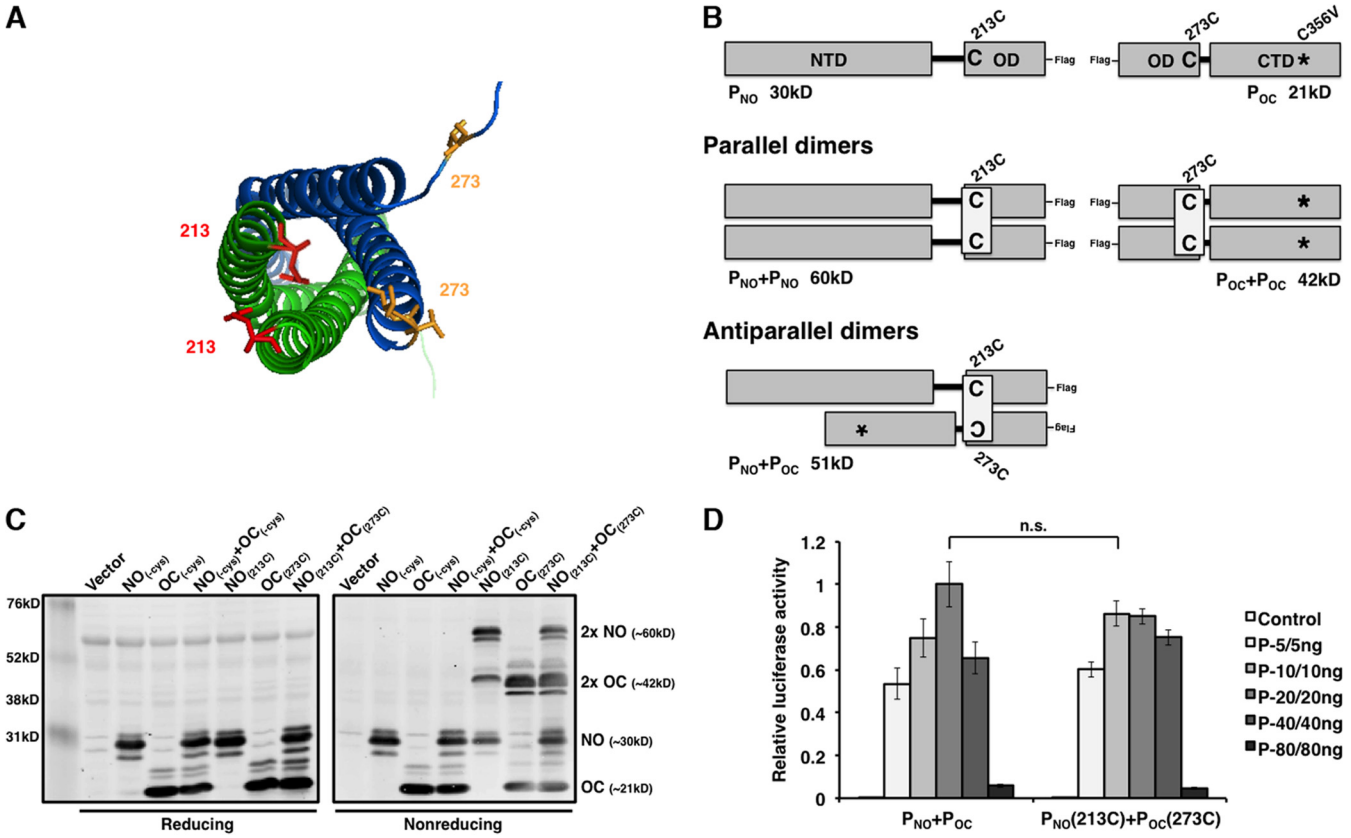

FIG 4 P mutants with engineered cysteine residues dimerize in parallel orientation with biological activity. (A) Pairs of parallel chains are shown in green or blue. Side chains of mutated amino acids 213 (red) and 273 (yellow) are highlighted. The amino acid 213 residue not contained in the file was superimposed from the adjacent parallel chain. The figure was generated using the PyMOL program (43). (B) Schematic representation of incorporated cysteine residues for disulfide bond engineering. The sizes of the dimers in the parallel and antiparallel orientations are provided. (C) Assessment of the parallel oligomerization status of P deletion mutants containing cysteine residues under reducing and nonreducing conditions. (D) Minigenome activity of engineered P deletion mutants. Increasing amounts of P mutants were transfected with other plasmids as described in Materials and Methods. *P* values were calculated using Student's *t* test. Error bars represent the SEMs of data from six replicates. n.s., not significant.

wild-type cysteine residue, a series of C356 mutants with mutations in full-length P and P_{OC} was generated and tested in the minigenome system in order to identify a mutation that maintains P function (Fig. 3A and B). P-C356V maintained the highest activity among the cysteine mutants; therefore, this modification was incorporated for all remaining P alterations.

P_O is defined as residues 213 to 277 (16). To determine if P forms parallel dimers, residues Q213 and V273 were changed to cysteine residues on the basis of the crystal structure of the oligomerization domain (Fig. 4A). P_{NO} and P_{OC} could be differentiated by their sizes (Fig. 4B). 293T cells were transfected with plasmids expressing P_{NO} and P_{OC} that contained no cysteine residues or P_{NO} with a cysteine residue at position 213 ($P_{NO\text{-}213C}$) and $P_{OC\text{-}273C}$. Polypeptides were separated by SDS-PAGE analysis under reducing and nonreducing conditions and detected by immunoblotting (Fig. 4C). As expected, only monomers were detected for P_{NO} (30 kDa) and P_{OC} (21 kDa) in all denaturing gels. Transfection with $P_{NO\text{-}213C}$ and $P_{OC\text{-}273C}$ resulted in bands corresponding to monomer and dimer ($2P_{NO}$, 60 kDa; $2P_{OC}$, 42 kDa) polypeptides. Bands with molecular masses higher than the molecular mass of a monomer were eliminated under reducing conditions, suggesting that oligomerization was due to disulfide bond formation (Fig. 4C). To confirm that the cysteine mutations maintain P function, $P_{NO\text{-}213C}$ and $P_{OC\text{-}273C}$ were tested in the minigenome system (Fig. 4D). Luciferase activity was similar for P_{NO}/P_{OC} and $P_{NO\text{-}213C}/P_{OC\text{-}273C}$, suggesting that addition of 213C and 273C does not disrupt P function. These results suggest that P forms parallel dimers.

Presence of antiparallel P molecules in a tetramer. In the P tetramer, the two pairs of parallel dimers are antiparallel to each other. The crystal structure of P_O was also utilized to strategically incorporate cysteine residues at possible sites of antiparallel interactions. It is important to note that a kink at Gly246 is found in only one molecule in the pair of parallel α helices, thus distinguishing interacting side chains of each parallel pair (Fig. 5A). The kink at Gly246 is responsible for structural differences between the antiparallel dimer pairs; therefore, in each antiparallel dimer pair, separate amino acid residues were identified as having side chains in close proximity. To determine if there are antiparallel P molecules with a kink or without a kink, cysteine residues were introduced at residues K241 and M248 or L243 and T250, respectively (Fig. 5B).

Cells were transfected with plasmids expressing P_{NO} and P_{OC} that contained no cysteine residues, $P_{NO\text{-}213C}$ and $P_{OC\text{-}273C}$ as parallel dimer controls, $P_{NO\text{-}241C}$, $P_{OC\text{-}248C}$, $P_{NO\text{-}243C}$, and $P_{OC\text{-}250C}$. Polypeptides were separated by SDS-PAGE analysis under reduc-

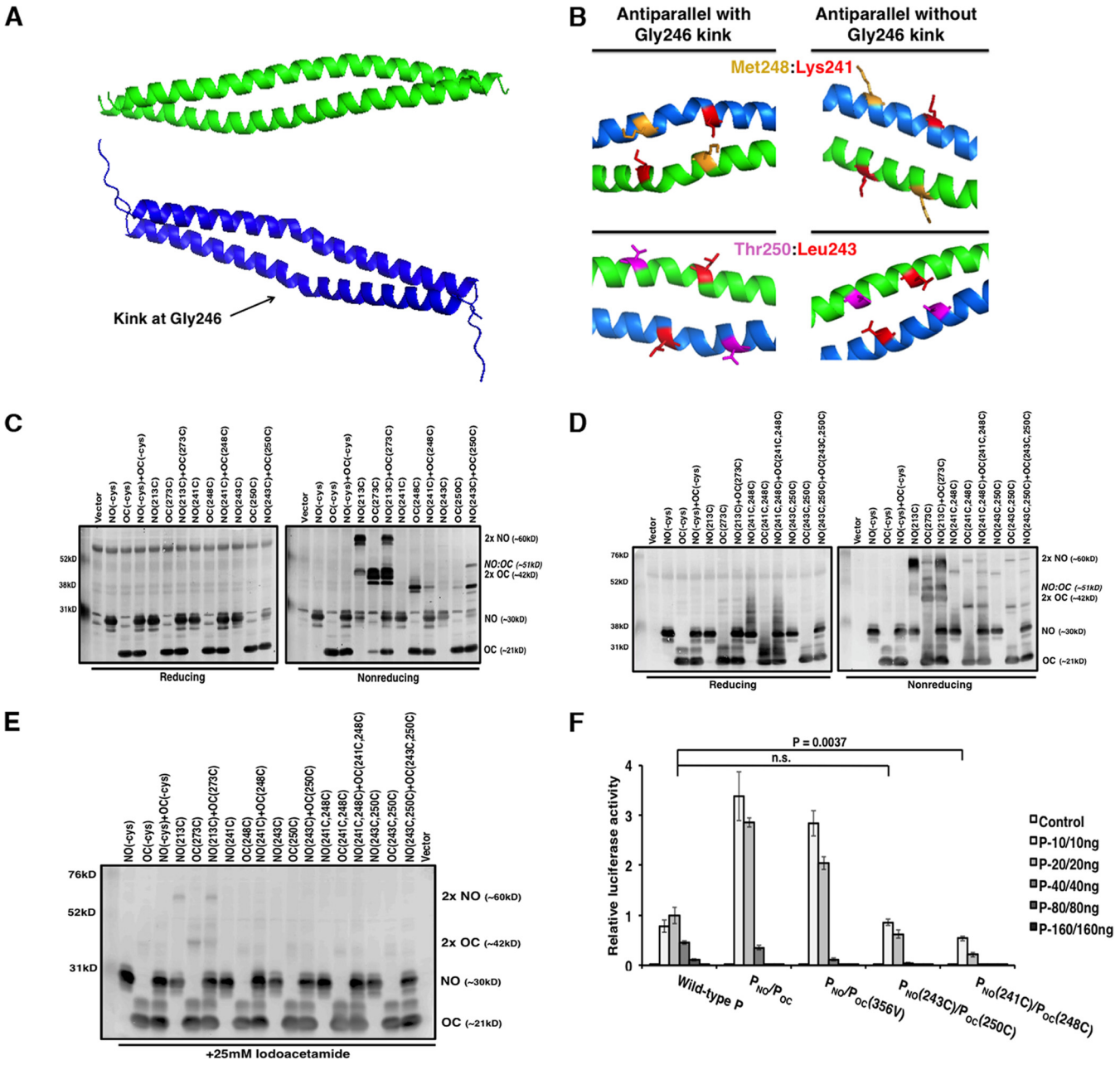

FIG 5 P mutants with engineered cysteine residues for cross-linking of antiparallel helices. (A and B) Pairs of antiparallel chains are shown in green or blue. The kink at Gly246 located on only one pair of helices is highlighted. (B) Residues with side chains in close proximity are highlighted. These residues were mutated to cysteine to engineer disulfide bonds between antiparallel α helices in chains containing and lacking the Gly246 kink. The figure was generated using the PyMOL program (43). (C and D) Assessment of the antiparallel oligomerization status of P deletion mutants containing single (C) or double (D) cysteine residues under reducing and nonreducing conditions. (E) Iodoacetamide treatment (25 mM) to achieve the natural dimerization orientation of P mutants with engineered parallel or antiparallel disulfide bonds. (F) Minigenome activity of engineered P mutants. Increasing amounts of P mutants were transfected with other plasmids as described in Materials and Methods. *P* values were calculated using Student's *t* test. Error bars represent the SEMs of data from six replicates.

ing and nonreducing conditions and detected by immunoblotting (Fig. 5C). Cotransfection with $P_{NO\text{-}243C}$ and $P_{OC\text{-}250C}$ resulted in the separation of an additional band whose size corresponded to that of a P_{NO}-P_{OC} antiparallel dimer (51 kDa). Since each pair of cysteine residues forms only a single disulfide bond, cysteine pairs were incorporated into each set of P truncations and polypeptides were examined to see if a cross-linked tetramer could be detected (Fig. 5D). Cotransfection with $P_{NO\text{-}241C,248C}$ and $P_{OC\text{-}241C,248C}$ also resulted in separation of an additional band whose size corresponded to that of a P_{NO}-P_{OC} antiparallel dimer. Extra bands corresponding to oligomer populations likely due to nonspecific interactions between the additional cysteine residues were observed. Even though the higher-molecular-mass bands were eliminated in Fig. 5C and D under reducing conditions, cell lysates were treated with iodoacetamide to confirm disulfide bond formation between dimers in their native conformation. As seen in Fig. 5E, only poly-

peptides corresponding to parallel dimers were observed for $P_{NO\text{-}213C}$ and $P_{OC\text{-}273C}$.

To confirm that the putative antiparallel cysteine mutations maintain P function, mutants with these mutations were tested in the minigenome system (Fig. 5F). Luciferase activity was reduced for the cysteine mutants; however, activity was still observed, indicating that incorporation of cysteine residues at these sites may hinder but not eliminate P function. The activity of $P_{NO\text{-}241C}$ and $P_{OC\text{-}248C}$ was comparable to that of P_{NO} and $P_{OC\text{-}248C}$ (data not shown). These results suggest that even though the incorporated antiparallel cysteine residues can interact to form disulfide bonds, the P oligomerization domain preferentially polymerizes to form functional parallel dimers before formation of a more dynamic tetramer.

Charged P_O zipper residues critical for P function. To validate the amino acid residues critical for tetramer formation, we examined residues likely to disrupt the parallel and antiparallel associations of the P subunits. The crystal structure of P_O revealed that the tetramer is primarily formed with hydrophobic interactions and two zippers of charged side chain interactions formed by Asp229, Glu236, and Asp240 (chain A) and by Arg231 and Lys238 (chain B) between the parallel pair of helices and by Lys253 and Lys260 (chain B) and by Asp229, Glu236, and Asp240 (chain B′) between the antiparallel pair of helices (16). To examine the roles of these residues in viral RNA synthesis, Arg231 and Lys238 were mutated to alanine to disrupt the charge interactions between the pair of parallel helices, Lys253 and Lys260 were mutated to alanine to disrupt the charge interactions between the pair of antiparallel helices, and the constructs were tested in the minigenome system. Disruption of the charged zipper interactions resulted in significantly reduced activity and completely abolished the activity for the mutant with Lys253Ala (Fig. 6A). The expression levels of P and NP were determined using immunoblotting (Fig. 6B).

MuV P_C contains a putative L-binding site. To determine the putative L-binding site within P, P deletion mutants were utilized. In order to investigate L binding within each individual P domain, P chimeras were generated with the corresponding regions of parainfluenza virus type 5 (PIV5), the virus most closely related to MuV, to enhance the structural stability of the MuV P domains (Fig. 7A). Visualization of full-length MuV L expression was limited; therefore, L deletion mutants were generated. The N-terminal residues of the L proteins of related viruses have been found to be essential for P binding; therefore, a sequence alignment of these L proteins with MuV L was analyzed to generate a MuV L truncation consisting of domains I through III ($L_{dI\text{-}III}$; aa 1 to 914) (data not shown) (32–35). Interactions between the P chimeras and MuV L were examined using coimmunoprecipitation of transfected 293T cells. The radioactively labeled cell lysates were immunoprecipitated with anti-MuV-P (full-length MuV P), anti-PIV5-P (full-length PIV5 P), anti-Flag (chimeric P truncations), or anti-HA ($L_{dI\text{-}III}$). As shown in Fig. 7B, only chimeras containing the C-terminal domain of MuV P interacted with $L_{dI\text{-}III}$. Coimmunoprecipitation was observed when both the P constructs or $L_{dI\text{-}III}$ was immunoprecipitated, suggesting that the C-terminal domain of MuV P interacted with $L_{dI\text{-}III}$. It is important to note that the coimmunoprecipitation band corresponding to full-length PIV5 P is not above the background, suggesting that PIV5 P does not interact with MuV $L_{dI\text{-}III}$. These results demonstrate that the C-terminal domain of MuV P interacts with $L_{dI\text{-}III}$.

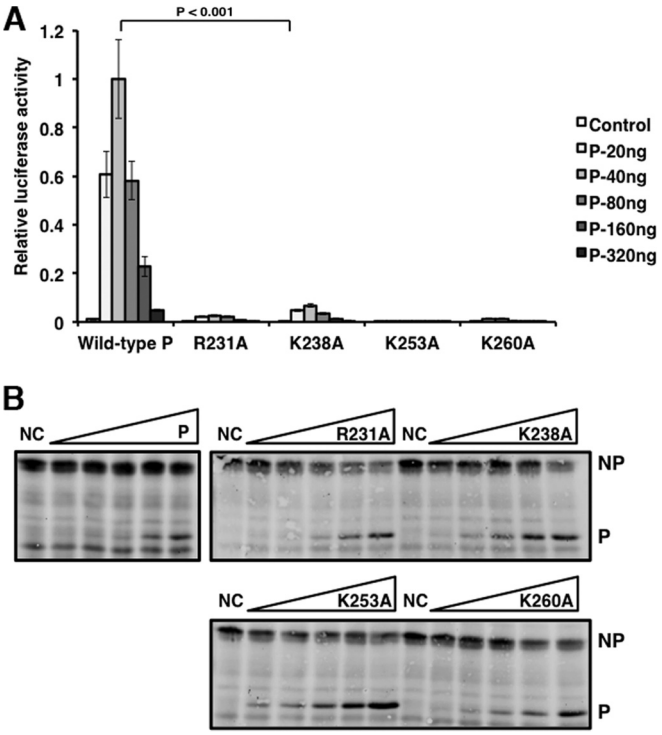

FIG 6 Charged residues in the P oligomerization domain are critical for P activity in the minigenome system. (A) Residues found in charged zippers were mutated to alanine and tested in the minigenome system. Increasing amounts of P mutants were transfected with other plasmids as described in Materials and Methods. *P* values were calculated using Student's *t* test. Error bars represent the SEMs of data from six replicates. (B) Immunoblotting was performed to detect the expression levels of NP, P, and the P mutants. NC, negative control (no P).

DISCUSSION

The P proteins of paramyxoviruses have a modular structure, and it is thought that the individual P domains can be modified or deleted without affecting the function of the other P domains (5). The MuV P domains have been systematically mapped and characterized (16). In this study, we generated P truncations to examine the function of the P domains in viral RNA synthesis. Previously, we found that transfecting additional P_N with full-length P resulted in enhanced activity in the MuV minigenome system due to uncoiling of the nucleocapsid (28). In the present study, we confirmed that all P domains are required for full P function. P multimerization has been found to be essential for viral transcription of rinderpest virus and VSV (10, 19). Interestingly, when MuV P truncations lacking either the N-terminal domain (P_{OC}) or the C-terminal domain (P_{NO}) were transfected together, P activity was restored due to *trans*-complementation through P_O. Thus, P multimerization via the central oligomerization domain is likely required for MuV P to function in viral RNA synthesis.

The crystal structure of MuV P_O revealed the formation of a tetramer consisting of two pairs of parallel α helices that are antiparallel to each other (16). It is unknown whether MuV P favorably forms parallel or antiparallel dimers during oligomerization. To further characterize the P oligomerization structure during viral RNA synthesis, the preferential α-helical orientation of P dimers was examined using engineered disulfide bond cross-linking. The introduction of cysteine residue pairs for cross-linking

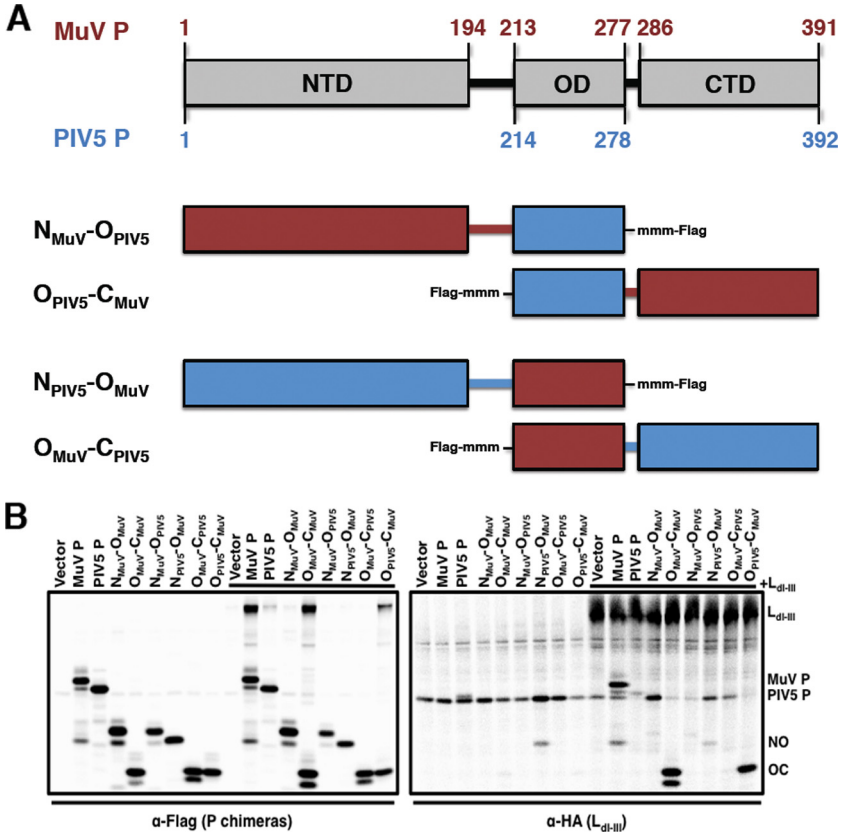

FIG 7 The C-terminal domain of P binds to L. (A) A schematic representation of the predicted amino acid residues for PIV5 P_N, P_O, and P_C from sequence analysis with MuV P is provided. Mutant names correspond to the domains included in the P deletion mutants. The terminal Flag tag locations as well as additional methionine residues (mmm), used to aid with visualization by radioactive labeling with ^{35}S, are included for each mutant. (B) Interaction between P domains and $L_{dI\text{-}III}$ in 293T cells. Cells were transfected with full-length P, P chimeras, or $L_{dI\text{-}III}$ or cotransfected with P and $L_{dI\text{-}III}$ and labeled with ^{35}S. Cell lysates were precleared with Sepharose G beads and coimmunoprecipitated with monoclonal anti-MuV P (full-length MuV P), anti-PIV5 P (full-length PIV5 P), anti-Flag (chimeric P truncations), or anti-HA ($L_{dI\text{-}III}$) antibody and resolved on a 12.5% SDS-polyacrylamide gel.

analysis is an applicable strategy for examination of protein structures. MuV P residues were strategically mutated to cysteine on the basis of the close proximity of side chains found in either the parallel or the antiparallel orientation of the crystal structure (Fig. 4 and 5). Our studies showed that P dimerization was preferentially parallel and these mutants were biologically active in the MuV minigenome. The selected antiparallel residues did not always cross-link antiparallel molecules, which resulted in reduced minigenome activity, possibly because mutation of these residues disrupted the native P structure. However, when multimerization was investigated with the addition of iodoacetamide, parallel dimers were observed, thus suggesting that disulfide bonds can readily form between the parallel helices. The cross-link between antiparallel molecules was not clearly observed in several cases, suggesting that the tetramer may be a more dynamic complex or the selection of the cysteine mutations was not appropriate. However, tetramer formation is required for P activity, as supported by the findings of mutational studies of the charge zippers (Fig. 6A).

A necessity of phosphorylation for oligomerization differs between P proteins. Phosphorylation of P is required for multimerization of the rhabdoviruses VSV and Chandipura virus and the more closely related paramyxovirus respiratory syncytial virus (11, 18, 36–38). The oligomerization of unphosphorylated P proteins expressed in bacteria suggests that phosphorylation is not required, as has been shown for rinderpest virus (10). Phosphorylation has also been found to be dispensable for P oligomerization of MuV, SeV, and measles virus (5, 9). We previously screened the serine and threonine (S/T) residues of MuV P to determine the phosphorylated residues critical for viral transcription and replication. Unexpectedly, six of the nine identified residues are located in the oligomerization domain (T250, S257, T258, T261, T262, and T265) (30). Analysis of these amino acids within the crystallized MuV P_O structure revealed that all six side chains are positioned outward to the tetramer; thus, it is unlikely that these residues are important for oligomerization and instead they are more accessible to interactions with host proteins, such as kinases. Further analysis of the phosphorylation of these S/T residues is ongoing.

We found a putative binding site of L to be in the C-terminal domain of P. Alterations of MuV L were required for the visualization of protein expression in our assays. The N-terminal 1,147 residues of the SeV L protein ($L_{dI\text{-}IV}$) were found to bind to SeV P; however, shorter truncations abolished P binding (32). Similarly, for PIV5, human PIV3, and measles virus, P binds to the N-terminal portion of L, with the shortest truncation of L being from measles virus, which included the 408 amino acids through domain I (34, 39, 40). An alignment of the sequences of these L proteins with the MuV L sequence was analyzed to generate MuV

L truncations consisting of domains I through III (aa 1 to 914), domains II through VI (aa 506 to 2261), and domains IV through VI (aa 882 to 2261) (35, 41). Visualization of L deletion mutant expression was achieved only for $L_{dI\text{-}III}$. The generation of truncations of L and P to determine binding sites may cause misfolding of the viral proteins. Additional binding sites within P may be unidentified because the failure of P domains to bind to L in our studies may be a result of structural changes rather than the deletion of putative binding sites. It is important to note that the C-terminal domain of MuV P alone was unable to coimmunoprecipitate with $L_{dI\text{-}III}$; therefore, the P sequences of PIV5, the virus most closely related to mumps virus, were utilized to stabilize MuV P-domain structures. Further studies are needed to more precisely locate the L-binding residues in P_C.

The oligomerization of MuV P results in two parallel dimers that are in an antiparallel orientation to each other during tetramer formation. This unique tetramer alignment likely has functional significance. Both the N-terminal and C-terminal domains of P bind to the nucleocapsid, and it has been proposed that P oligomerization brings the terminal regions together in close proximity for effective nucleocapsid binding (16). Our studies reveal that the N-terminal and C-terminal domains of P can *trans*-complement each other to achieve functional activity in a minigenome system, likely through oligomerization of the P truncations. A cartwheel model has been proposed from studies with SeV, where P is thought to simultaneously make and break contacts with the nucleocapsid to ensure polymerase processivity during viral RNA synthesis (42). This model also proposes that binding of P to the nucleocapsid or L may open the RNP structure so that the polymerase can access the viral template. Recent studies with MuV have shown that the nucleocapsid uncoils to expose the RNA access to the polymerase through an interaction between the N-terminal domain of P and the nucleocapsid (28). Our studies suggest that MuV P is able to place the polymerase complex on the NP-RNA template via an L-binding site in the C-terminal domain of P.

ACKNOWLEDGMENTS

We appreciate the helpful discussions and technical assistance from all members of Biao He's laboratory.

This work was supported by grants (R01AI097368 and R01AI106307) from the National Institutes of Health.

REFERENCES

1. **Carbone KM, Wolinsky JS.** 2001. Mumps virus, p 1381–1441. *In* Knipe DM, Howley PM, Griffin DE, Lamb RA, Martin MA, Roizman B, Straus SE (ed), Fields virology, 4th ed. Lippincott Williams & Wilkins, Philadelphia, PA.
2. **Emerson S, Yu Y.** 1975. Both NS and L proteins are required for in vitro RNA synthesis by vesicular stomatitis virus. J Virol **15:**1348–1356.
3. **Lamb RA, Kolakofsky D.** 2001. Paramyxoviridae: the viruses and their replication, p 1305–1340. *In* Knipe DM, Howley PM, Griffin DE, Lamb RA, Martin MA, Roizman B, Straus SE (ed), Fields virology, 4th ed. Lippincott Williams & Wilkins, Philadelphia, PA.
4. **Banerjee AK, Barik S, De BP.** 1991. Gene expression of nonsegmented negative strand RNA viruses. Pharmacol Ther **51:**47–70. http://dx.doi.org/10.1016/0163-7258(91)90041-J.
5. **Curran J, Boeck R, Lin-Marq N, Lupas A, Kolakofsky D.** 1995. Paramyxovirus phosphoproteins form homotrimers as determined by an epitope dilution assay, via predicted coiled coils. Virology **214:**139–149. http://dx.doi.org/10.1006/viro.1995.9946.
6. **Tarbouriech N, Curran J, Ruigrok RWH, Burmeister WP.** 2000. Tetrameric coiled coil domain of Sendai virus phosphoprotein. Nat Struct Biol **7:**777–781.
7. **Smallwood S, Ryan KW, Moyer SA.** 1994. Deletion analysis defines a carboxyl-proximal region of Sendai virus P protein that binds to the polymerase L protein. Virology **202:**154–163. http://dx.doi.org/10.1006/viro.1994.1331.
8. **Curran J, Pelet T, Kolakofsky D.** 1994. An acidic activation-like domain of the Sendai virus P protein is required for RNA synthesis and encapsidation. Virology **202:**875–884. http://dx.doi.org/10.1006/viro.1994.1409.
9. **Kolakofsky D, Le Mercier P, Iseni F, Garcin D.** 2004. Viral RNA polymerase scanning and the gymnastics of Sendai virus RNA synthesis. Virology **318:**463. http://dx.doi.org/10.1016/j.virol.2003.10.031.
10. **Rahaman A, Srinivasan N, Shamala N, Shaila MS.** 2004. Phosphoprotein of the rinderpest virus forms a tetramer through a coiled coil region important for biological function: a structural insight. J Biol Chem **279:**23606–23614. http://dx.doi.org/10.1074/jbc.M400673200.
11. **Asenjo A, Villanueva N.** 2000. Regulated but not constitutive human respiratory syncytial virus (HRSV) P protein phosphorylation is essential for oligomerization. FEBS Lett **467:**279–284. http://dx.doi.org/10.1016/S0014-5793(00)01171-6.
12. **Castagne N, Barbier A, Bernard J, Rezaei H, Huet J-C, Henry C, Da Costa B, Eleouet J-F.** 2004. Biochemical characterization of the respiratory syncytial virus P-P and P-N protein complexes and localization of the P protein oligomerization domain. J Gen Virol **85:**1643–1653. http://dx.doi.org/10.1099/vir.0.79830-0.
13. **Chattopadhyay S, Banerjee AK.** 2009. Phosphoprotein, P of human parainfluenza virus type 3 prevents self-association of RNA-dependent RNA polymerase, L. Virology **383:**226–236. http://dx.doi.org/10.1016/j.virol.2008.10.019.
14. **Leyrat C, Renner M, Harlos K, Grimes JM.** 2013. Solution and crystallographic structures of the central region of the phosphoprotein from human metapneumovirus. PLoS One **8:**e80371. http://dx.doi.org/10.1371/journal.pone.0080371.
15. **Communie G, Crépin T, Maurin D, Jensen MR, Blackledge M, Ruigrok RWH.** 2013. Structure of the tetramerization domain of measles virus phosphoprotein. J Virol **87:**7166–7169. http://dx.doi.org/10.1128/JVI.00487-13.
16. **Cox R, Green TJ, Purushotham S, Deivanayagam C, Bedwell GJ, Prevelige PE, Luo M.** 2013. Structural and functional characterization of the mumps virus phosphoprotein. J Virol **87:**7558–7568. http://dx.doi.org/10.1128/JVI.00653-13.
17. **Ding HT, Green TJ, Lu SY, Luo M.** 2006. Crystal structure of the oligomerization domain of the phosphoprotein of vesicular stomatitis virus. J Virol **80:**2808–2814. http://dx.doi.org/10.1128/JVI.80.6.2808-2814.2006.
18. **Gao Y, Lenard J.** 1995. Cooperative binding of multimeric phosphoprotein (P) of vesicular stomatitis virus to polymerase (L) and template: pathways of assembly. J Virol **69:**7718–7723.
19. **Chen M, Ogino T, Banerjee AK.** 2006. Mapping and functional role of the self-association domain of vesicular stomatitis virus phosphoprotein. J Virol **80:**9511–9518. http://dx.doi.org/10.1128/JVI.01035-06.
20. **Ivanov I, Crépin T, Jamin M, Ruigrok RWH.** 2010. Structure of the dimerization domain of the rabies virus phosphoprotein. J Virol **84:**3707–3710. http://dx.doi.org/10.1128/JVI.02557-09.
21. **Chenik M, Schnell M, Conzelmann KK, Blondel D.** 1998. Mapping the interacting domains between the rabies virus polymerase and phosphoprotein. J Virol **72:**1925–1930.
22. **Schoehn G, Iseni F, Mavrakis M, Blondel D, Ruigrok RWH.** 2001. Structure of recombinant rabies virus nucleoprotein-RNA complex and identification of the phosphoprotein binding site. J Virol **75:**490–498. http://dx.doi.org/10.1128/JVI.75.1.490-498.2001.
23. **Mavrakis M, Méhouas S, Réal E, Iseni F, Blondel D, Tordo N, Ruigrok RWH.** 2006. Rabies virus chaperone: identification of the phosphoprotein peptide that keeps nucleoprotein soluble and free from non-specific RNA. Virology **349:**422–429. http://dx.doi.org/10.1016/j.virol.2006.01.030.
24. **Ryan KW, Kingsbury DW.** 1988. Carboxyl-terminal region of Sendai virus P protein is required for binding to viral nucleocapsids. Virology **167:**106–112. http://dx.doi.org/10.1016/0042-6822(88)90059-1.
25. **García-Barreno B, Delgado T, Melero JA.** 1996. Identification of protein regions involved in the interaction of human respiratory syncytial virus phosphoprotein and nucleoprotein: significance for nucleocapsid assembly and formation of cytoplasmic inclusions. J Virol **70:**801–808.
26. **De BP, Hoffman MA, Choudhary S, Huntley CC, Banerjee AK.** 2000. Role of NH_2- and COOH-terminal domains of the P protein of human

parainfluenza virus type 3 in transcription and replication. J Virol **74:** 5886–5895. http://dx.doi.org/10.1128/JVI.74.13.5886-5895.2000.
27. **Kingston RL, Baase WA, Gay LS.** 2004. Characterization of nucleocapsid binding by the measles virus and mumps virus phosphoproteins. J Virol **78:**8630–8640. http://dx.doi.org/10.1128/JVI.78.16.8630-8640.2004.
28. **Cox R, Pickar A, Qiu S, Tsao J, Rodenburg C, Dokland T, Elson A, He B, Luo M.** 2014. Structural studies on the authentic mumps virus nucleocapsid showing uncoiling by the phosphoprotein. Proc Natl Acad Sci U S A **111:**15208–15213. http://dx.doi.org/10.1073/pnas.1413268111.
29. **Xu P, Li Z, Sun D, Lin Y, Wu J, Rota PA, He B.** 2011. Rescue of wild-type mumps virus from a strain associated with recent outbreaks helps to define the role of the SH ORF in the pathogenesis of mumps virus. Virology **417:**126–136. http://dx.doi.org/10.1016/j.virol.2011.05.003.
30. **Pickar A, Xu P, Elson A, Li Z, Zengel J, He B.** 2014. Roles of serine and threonine residues of mumps virus P protein in viral transcription and replication. J Virol **88:**4414–4422. http://dx.doi.org/10.1128/JVI.03673-13.
31. **Xu P, Luthra P, Li Z, Fuentes S, D'Andrea JA, Wu J, Rubin S, Rota Pa, He B.** 2012. The V protein of mumps virus plays a critical role in pathogenesis. J Virol **86:**1768–1776. http://dx.doi.org/10.1128/JVI.06019-11.
32. **Chandrika R, Horikami SM, Smallwood S, Moyer SA.** 1995. Mutations in conserved domain I of the Sendai virus L polymerase protein uncouple transcription and replication. Virology **213:**352–363. http://dx.doi.org/10.1006/viro.1995.0008.
33. **Cevik B, Holmes DE, Vrotsos E, Feller JA, Smallwood S, Moyer SA.** 2004. The phosphoprotein (P) and L binding sites reside in the N-terminus of the L subunit of the measles virus RNA polymerase. Virology **327:** 297–306. http://dx.doi.org/10.1016/j.virol.2004.07.002.
34. **Parks GD.** 1994. Mapping of a region of the paramyxovirus L protein required for the formation of a stable complex with the viral phosphoprotein P. J Virol **68:**4862–4872.
35. **Sidhu MS, Menonna JP, Cook SD, Dowling PC, Udem SA.** 1993. Canine distemper virus L gene: sequence and comparison with related viruses. Virology **193:**50–65. http://dx.doi.org/10.1006/viro.1993.1102.
36. **Pattnaik AK, Hwang L, Li T, Englund N, Mathur M, Das T, Banerjee AK.** 1997. Phosphorylation within the amino-terminal acidic domain I of the phosphoprotein of vesicular stomatitis virus is required for transcription but not for replication. J Virol **71:**8167–8175.
37. **Raha T, Samal E, Majumdar A, Basak S, Chattopadhyay D, Chattopadhyay DJ.** 2000. N-terminal region of P protein of Chandipura virus is responsible for phosphorylation-mediated homodimerization. Protein Eng **13:**437–444. http://dx.doi.org/10.1093/protein/13.6.437.
38. **Barik S, McLean T, Dupuy LC.** 1995. Phosphorylation of Ser232 directly regulates the transcriptional activity of the P protein of human respiratory syncytial virus: phosphorylation of Ser237 may play an accessory role. Virology **213:**405–412. http://dx.doi.org/10.1006/viro.1995.0013.
39. **Malur AG, Choudhary SK, De BP, Banerjee AK.** 2002. Role of a highly conserved NH_2-terminal domain of the human parainfluenza virus type 3 RNA polymerase. J Virol **76:**8101–8109. http://dx.doi.org/10.1128/JVI.76.16.8101-8109.2002.
40. **Horikami SM, Smallwood S, Bankamp B, Moyer SA.** 1994. An amino-proximal domain of the L protein binds to the P protein in the measles virus RNA polymerase complex. Virology **205:**540–545. http://dx.doi.org/10.1006/viro.1994.1676.
41. **Poch O, Blumberg BM, Bougueleret L, Tordo N.** 1990. Sequence comparison of five polymerases (L proteins) of unsegmented negative-strand RNA viruses: theoretical assignment of functional domains. J Gen Virol **71:**1153–1162. http://dx.doi.org/10.1099/0022-1317-71-5-1153.
42. **Curran J.** 1998. A role for the Sendai virus P protein trimer in RNA synthesis. J Virol **72:**4274–4280.
43. **Delano W.** 2002. The PyMOL user's manual. Delano Scientific, San Carlos, CA.